Broadband and robust optical waveguide devices using coherent tunnelling adiabatic passage

Kelvin Chung,[1,*] Timothy J. Karle,[1] Masum Rab,[1] Andrew D. Greentree,[1,2] and Snjezana Tomljenovic-Hanic[1]

[1]*School of Physics, The University of Melbourne, Parkville, Victoria 3010, Australia*
[2]*Applied Physics, School of Applied Sciences, RMIT University, Melbourne, Victoria 3001, Australia*
[*]*kelvinc@student.unimelb.edu.au*

Abstract: We numerically demonstrate an optical waveguide structure for the coherent tunnelling adiabatic passage of photons. An alternative coupling scheme is used compared to earlier work. We show that a three rib optical waveguide structure is robust to material loss in the intermediate waveguide and variations to the waveguide parameters. We also present a five rib optical waveguide structure that represents a new class of octave spanning power divider.

OCIS codes: (230.0230) Optical devices; (230.7390) Waveguides, planar.

References and links

1. S. Longhi, M. Marangoni, D. Janner, R. Ramponi, P. Laporta, E. Cianci, and V. Foglietti, "Observation of wave packet dichotomy and adiabatic stabilization in an optical waveguide," Phys. Rev. Lett. **94**, 073002 (2005).
2. S. Longhi, "Adiabatic passage of light in coupled optical waveguides," Phys. Rev. E **73**, 026607 (2006).
3. S. Longhi, "Optical realization of multilevel adiabatic population transfer in curved waveguide arrays," Phys. Lett. A **359**, 166–170 (2006).
4. E. Paspalakis, "Adiabatic three-waveguide directional coupler," Opt. Commun. **258**, 30–34 (2006).
5. S. Longhi, G. Della Valle, M. Ornigotti, and P. Laporta, "Coherent tunneling by adiabatic passage in an optical waveguide system," Phys. Rev. B **76**, 201101 (2007).
6. G. Della Valle, M. Ornigotti, T. Fernandez, P. Laporta, S. Longhi, A. Coppa, and V. Foglietti, "Adiabatic light transfer via dressed states in optical waveguide arrays," Appl. Phys. Lett. **92**, 011106 (2008).
7. R. Sapienza, P. Costantino, D. Wiersma, M. Ghulinyan, C. J. Oton, and L. Pavesi, "Optical analogue of electronic bloch oscillations," Phys. Rev. Lett. **91**, 263902 (2003).
8. D. N. Christodoulides, F. Lederer, and Y. Silberberg, "Discretizing light behaviour in linear and nonlinear waveguide lattices," Nature **424**, 817–823 (2003).
9. H. Trompeter, T. Pertsch, F. Lederer, D. Michaelis, U. Streppel, A. Bräuer, and U. Peschel, "Visual observation of zener tunneling," Phys. Rev. Lett. **96**, 023901 (2006).
10. S. Longhi, "Quantum-optical analogies using photonic structures," Laser Photon. Rev. **3**, 243–261 (2009).
11. K. Bergmann, H. Theuer, and B. W. Shore, "Coherent population transfer among quantum states of atoms and molecules," Rev. Mod. Phys. **70**, 1003–1025 (1998).
12. N. V. Vitanov, T. Halfmann, B. W. Shore, and K. Bergmann, "Laser-induced population transfer by adiabatic passage techniques," Annu. Rev. Phys. Chem. **52**, 763–809 (2001).
13. A. D. Greentree, J. H. Cole, A. R. Hamilton, and L. C. L. Hollenberg, "Coherent electronic transfer in quantum dot systems using adiabatic passage," Phys. Rev. B **70**, 235317 (2004).
14. K. Eckert, M. Lewenstein, R. Corbalán, G. Birkl, W. Ertmer, and J. Mompart, "Three-level atom optics via the tunneling interaction," Phys. Rev. A **70**, 023606 (2004).
15. M. Rab, J. H. Cole, N. G. Parker, A. D. Greentree, L. C. L. Hollenberg, and A. M. Martin, "Spatial coherent transport of interacting dilute bose gases," Phys. Rev. A **77**, 061602 (2008).

#171934 - $15.00 USD Received 4 Jul 2012; revised 7 Sep 2012; accepted 7 Sep 2012; published 24 Sep 2012

16. J. D. Joannopoulos, R. D. Meade, and J. N. Winn, *Photonic Crystals: Molding the Flow of Light* (Princeton University Press, 1995).
17. K. Okamoto, *Fundamentals of optical waveguides* (Academic Press, 2000).
18. F. Dreisow, M. Ornigotti, A. Szameit, M. Heinrich, R. Keil, S. Nolte, A. Tunnermann, and S. Longhi, "Polychromatic beam splitting by fractional stimulated raman adiabatic passage," Appl. Phys. Lett. **95**, 261102 (2009).
19. A. A. Rangelov, N. V. Vitanov, "Achromatic multiple beam splitting by adiabatic passage in optical waveguides," Phys. Rev. A **85**, 055803 (2012).
20. A. D. Greentree, S. J. Devitt, and L. C. L. Hollenberg, "Quantum-information transport to multiple receivers," Phys. Rev. A **73**, 032319 (2006).
21. S. J. Devitt, A. D. Greentree, and L. C. L. Hollenberg, "Information free quantum bus for generating stabiliser states." Quantum Inf. Process. **6**, 229–242 (2007).
22. C. D. Hill, A. D. Greentree, and L. C. L. Hollenberg, "Parallel interaction-free measurement using spatial adiabatic passage," New J. Phys. **13**, 125002 (2011).
23. B. E. Little and W. P. Huang, "Coupled-mode theory for optical waveguides," Prog. Electromagn. Res. **10**, 217–270 (1995).
24. S. Longhi, "Photonic transport via chirped adiabatic passage in optical waveguides," J. Phys. B: At., Mol. Opt. Phys. **40**, F189 (2007).
25. T. Tamir, *Integrated Optics, Topics in Applied Physics, Vol. 7* (Springer, 1979).
26. L. M. Jong, A. D. Greentree, V. I. Conrad, L. C. L. Hollenberg, and D. N. Jamieson, "Coherent tunneling adiabatic passage with the alternating coupling scheme," Nanotechnology **20**, 405402 (2009).
27. J. H. Cole, A. D. Greentree, L. C. L. Hollenberg, and S. Das Sarma, "Spatial adiabatic passage in a realistic triple well structure," Phys. Rev. B **77**, 235418 (2008).

1. Introduction

Optical waveguide systems have been connected to a variety of coherent quantum effects that occur in atomic, molecular and condensed matter systems such as: adiabatic stabilisation [1], coherent population transfer [2–6], Bloch oscillations [7, 8] and Zener tunnelling [9]. These coherent quantum effects are often difficult to explore in atomic, molecular and condensed matter systems because of effects such as many-body interactions, decoherence and the presence of time-dependent/non-linear terms in the Schrödinger equation. In the realm of guided-wave optics, one is able to obtain a direct realisation of the dynamics of a coherent quantum system, described by a tailored Hamiltonian, by mimicking laser and matter interactions with geometrical bending of the optical waveguide structure [10].

Another example of a coherent quantum effect is STImulated RAman Adiabatic Passage (STIRAP) [11, 12], which is the coherent transport of population within an atomic or molecular system. The spatial analogue to STIRAP is known as Coherent Tunnelling Adiabatic Passage (CTAP) [13]. Applying CTAP methods to optical waveguides provides a new set of tools for the design of photonic devices, and this is the main theme of the present work.

CTAP has been proposed in the condensed matter regime for the transport *in space* of electrons between quantum dots [13], neutral atoms within optical traps [14] and Bose-Einstein condensates [15]. Research in optical waveguide CTAP devices has steadily increased due to the relative ease of engineering optical structures compared to solid state systems [10]. A comparison between the Schrödinger equation (quantum) and Helmholtz equation (guided-wave optics) reveals an analogy between the quantised energy levels and discretised guided modes of an optical waveguide [16, 17]. The ideas of adiabatic passage of photons using optical waveguides have been theoretically proposed in three-core [2, 4], multiple arrays [3, 6] and experimentally realised for a three-waveguide system [5]. Optical waveguide CTAP structures offer broadband beam splitting [18, 19]. The experimental realisation of optical waveguide CTAP enables exploration of the parameter space of condensed matter CTAP systems using appropriate mappings between both regimes. This mapping accurately allows us to implement other adiabatic quantum processes to optical waveguide systems.

We introduce a three optical waveguide structure that demonstrates CTAP for photons, using a different coupling scheme from previous work utilising Gaussian profiles [2, 5, 6]. The

#171934 - $15.00 USD Received 4 Jul 2012; revised 7 Sep 2012; accepted 7 Sep 2012; published 24 Sep 2012

background theory and methodology in the design process can be found in Sec. 2. Our scheme results in a length reduction of one order of magnitude compared with previous work, making our approach more useful for practical devices. The propagation behaviour for this structure can be found in Sec. 3.1. The three waveguide structure shows remarkable robustness in the transport of light when material loss (i.e. imaginary refractive index) is introduced to the central waveguide and when the rib heights of constituent waveguides are changed from the optimised system, the results can be found in sections 3.2 and 3.3 respectively. The transmission response from the variation of the rib heights produced qualitative agreement with previous work done in related approaches (cf. [12, 13]).

Extending on the ideas of the three waveguide structure, we also introduce a new class of power divider consisting of five waveguides, based on Multiple Recipient Adiabatic Passage [20–22] (MRAP) with the propagation results found in Sec. 3.4. This five waveguide structure has a very broadband spectral response and is shown in Sec. 3.5. The robust nature of the power divider allows for applications that include coupling power between different materials systems, across interfaces, taking advantage of the low field strength in the intermediate waveguides.

2. Theory and method

The archetypal CTAP system consists of 3 basis position eigenstates of $|1\rangle$,$|2\rangle$,$|3\rangle$, where the goal of CTAP is to have robust population transfer from an initial state $|1\rangle$ to final state $|3\rangle$ and a consequence of this transport method is the minimal occupation of the intermediate state $|2\rangle$ [13]. The basis states represent spatial wavefunctions in the quantum realm and are analogous to optical modes that exist in waveguides for guided-wave optics. These modes are characterised by propagation constants, β. The propagation constant is analogous to the energy when mapping between the Helmholtz and Schrödinger equations [16]. The Hamiltonian that governs the CTAP system is a 3×3 matrix with off-diagonal terms that correspond to the coherent tunnelling rates, between adjacent site pairs of $|1\rangle,|2\rangle$ and $|2\rangle,|3\rangle$. The coupled differential equation and coupling coefficient matrix for a three-waveguide implementation of CTAP is [4, 5]:

$$-i\frac{d}{dz}\mathbf{A}(z)=\mathbf{C}(z)\mathbf{A}(z), \qquad \mathbf{C}(z)=\begin{bmatrix} 0 & -\kappa_{12}(z) & 0 \\ -\kappa_{12}(z) & -\Delta_{21} & -\kappa_{23}(z) \\ 0 & -\kappa_{23}(z) & -\Delta_{31} \end{bmatrix}, \tag{1}$$

where z is the propagation direction, $\mathbf{A}(z)=[a_1(z),a_2(z),a_3(z)]^{\mathrm{T}}$ is a vector representing field amplitudes of waveguides $|1\rangle,|2\rangle,|3\rangle$ respectively. $\mathbf{C}(z)$ is the overall coupling coefficient matrix. κ_{ab} are the coupling coefficients between adjacent waveguides. $\Delta_{ab}=\beta_a-\beta_b$ is the effective detuning, or equivalently the mode mismatch between waveguides a and b. Diagonalising $\mathbf{C}(z)$ leads to the identification of three supermodes. When $\Delta_{31}=0$, one of these is the equivalent of the dark state in STIRAP [12] and null state for CTAP [13]. We denote this supermode $\mathbf{E}(z)$ and it is a superposition solely of modes $|1\rangle$ and $|3\rangle$:

$$\mathbf{E}(z)=-\frac{\kappa_{23}(z)}{\sqrt{\kappa_{12}(z)^2+\kappa_{23}(z)^2}}\mathbf{E_1}+0\times\mathbf{E_2}+\frac{\kappa_{12}(z)}{\sqrt{\kappa_{12}(z)^2+\kappa_{23}(z)^2}}\mathbf{E_3}. \tag{2}$$

where $\mathbf{E}=\mathbf{A}(z)\exp[i(\beta z-\omega t)]$ is the electric field. Maintaining the system in this supermode achieves coherent and complete population transfer from $|1\rangle$ to $|3\rangle$ by adiabatic variation of the tunnelling rates through the counter-intuitive sequence [12]. For the counter-intuitive sequence, initially the coupling between the unpopulated states is much greater than that connecting the

#171934 - $15.00 USD Received 4 Jul 2012; revised 7 Sep 2012; accepted 7 Sep 2012; published 24 Sep 2012

populated state. In the optical waveguide setting, the tunnelling rates are the coupling coefficients between adjacent waveguides [2, 5, 24].

We choose rib waveguides (see Fig. 1(a)) because large evanescent fields can exist between waveguides to facilitate coupling. The refractive index of the surround region is the same as the rib region. For single mode operation we have chosen the rib, surround heights and core width to be $1.8, 1.0$ and $2.36\ \mu$m respectively, using the effective index method [25].

The refractive indices that constitute the rib waveguide are: $n_s = 1.45$ (SiO_2 substrate), $n_f = 1.56$ (polymer film) and $n_c = 1.0$ (air cover). Polymer is chosen as the guiding index due to the relative ease to fabricate rib waveguides from this material. The basic rib waveguide is designed to operate at $\lambda = 1.55\ \mu$m using standard beam propagation software (BeamPROP 8.2 by RSoft Design Group, Inc.). Using this basic rib waveguide, we designed 3- and 5-waveguide (CTAP and MRAP respectively) structures based on the following coupling coefficients between adjacent waveguides (labelled $|n\rangle$, where n is the waveguide number, see Fig. 1(b,c)).

$$\kappa_{12}(z) = (\kappa_{\max} - \kappa_{\min}) \sin^2\left(\frac{\pi z}{2L}\right) + \kappa_{\min}, \quad \kappa_{23}(z) = (\kappa_{\max} - \kappa_{\min}) \cos^2\left(\frac{\pi z}{2L}\right) + \kappa_{\min}, \quad (3)$$

where $\kappa_{\max}/\kappa_{\min}$ is maximum/minimum coupling coefficient [26], L is the total length. There is considerable flexibility in the coupling scheme provided that the chosen functions satisfy the adiabaticity criterion [11, 12, 27]. Previous work was done with Gaussian coupling [5].

The geometry of the CTAP and MRAP waveguide structures (see Fig. 1(b) and (c) respectively) is determined by calculating the propagation constants of the supermodes of a two optical waveguide system, i.e. a directional coupler. These βs are then used to calculate the coupling coefficients κ as a function of the gap between the two waveguides [23], which has the following form $\kappa = (\beta^+ - \beta^-)/2$; where $\beta^\pm$ are the propagation constants of the symmetric and antisymmetric supermodes respectively of the directional coupler. To design the full CTAP structures, κ is set to the CTAP protocol of Eqs. (3) to generate the geometry of the structures in the *xz*-plane (top view). In the results that follow, a scalar beam propagation method is used, i.e., without polarisation of the optical fields.

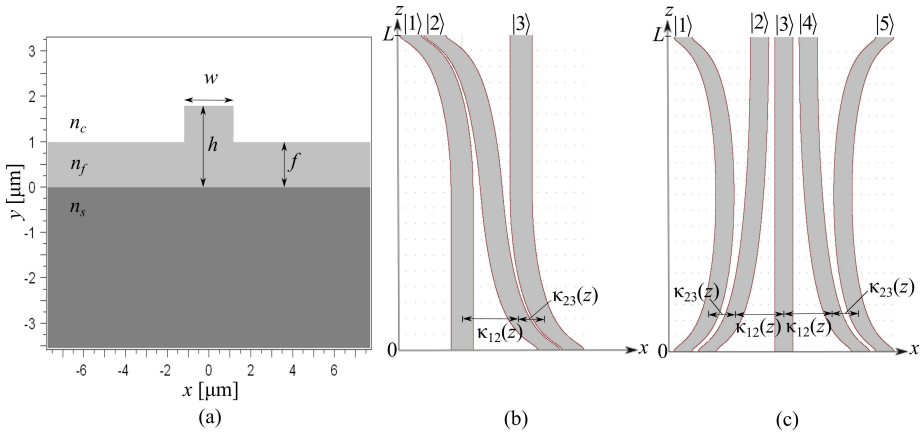

Fig. 1. (a) The basic rib waveguide (transverse slice, *xy*-plane) used to construct the CTAP and MRAP structures; where h, f, and w represent the rib, surround heights and core width respectively. n_c, n_f and n_s represent the refractive indices of the cladding, core and substrate respectively. (b) The CTAP optical structure (top view, *xz*-plane) and (c) MRAP optical structure (top view, *xz*-plane), with coupling coefficients of Eqs. (3) shown.

#171934 - $15.00 USD Received 4 Jul 2012; revised 7 Sep 2012; accepted 7 Sep 2012; published 24 Sep 2012

3. Results

3.1. 3-waveguide CTAP - propagation

For the CTAP structure we excite waveguide $|1\rangle$ at $z = 0$ (see Fig. 1(b)), which results in a counter-intuitive coupling sequence, with the fundamental mode of the basic waveguide. Figure 2(a) shows the top view (i.e. *xz*-plane) of the propagation of light through the CTAP structure. Figure 2(b) shows the power evolution through constituent waveguides of the CTAP structure. The length, L, is chosen such that light in waveguide $|2\rangle$ at any point along the structure is kept to a minimum.

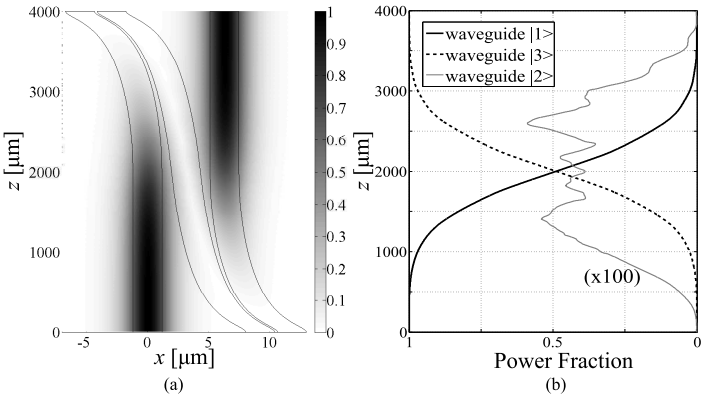

Fig. 2. Light propagation (using BeamPROP 8.2 by RSoft Design Group, Inc.) through the CTAP structure based on the coupling coefficients of the CTAP protocol, where (a) is the top view (*xz*-plane) of the structure and the black outlines represent the side walls of the individual waveguides. The grey scale represents the intensity of light, peak is normalised to 1. (b) The evolution of the power in each individual waveguide for the CTAP structure. The power in waveguide $|2\rangle$ has been multiplied by 100 to make it visible on this scale. Here we have set $\kappa_{\max} = 2 \times 10^{-2}\ \mu\text{m}^{-1}$, $\kappa_{\min} = 2 \times 10^{-5}\ \mu\text{m}^{-1}$ and the total length to $L = 4$ mm.

Figure 2 indicates that light is coupled across the structure from waveguide $|1\rangle$ to waveguide $|3\rangle$ with minimal excitation of waveguide $|2\rangle$, showing that light is adiabatically transported via the CTAP process. These results confirm previous work with three optical waveguide CTAP that used a Gaussian coupling scheme [5], which also showed that light primarily exists in the outer waveguides of the three waveguide CTAP system. The structure is one order of magnitude shorter, in length, with respect to previous work [5].

3.2. 3-waveguide CTAP - material loss in waveguide $|2\rangle$

Ordinarily, one might expect that large loss in any of the three waveguides might lead to a commensurate loss in performance for the entire device. However, the CTAP protocol minimises the power in waveguide $|2\rangle$, despite the light demonstrably travelling from $|1\rangle$ to $|3\rangle$ via $|2\rangle$, CTAP is incredibly insensitive to loss in $|2\rangle$.

We demonstrate this robustness by the introduction of an imaginary refractive index, n_i, for waveguide $|2\rangle$. Figure 3 shows the optical power loss as function of n_i for waveguide $|3\rangle$ in the CTAP structure (solid line) and waveguide $|2\rangle$ only (dash-dot line).

At $n_i = 1 \times 10^{-3}$, the power loss in waveguide $|2\rangle$ only is $\alpha_{|2\rangle} = -93.2$ dB and for the whole CTAP structure is $\alpha_{\text{CTAP}} = -0.71$ dB. These results indicate an approximate 10 order of magnitude difference in power loss when CTAP is used. Also at $n_i = 0.01$, the power loss for

#171934 - $15.00 USD Received 4 Jul 2012; revised 7 Sep 2012; accepted 7 Sep 2012; published 24 Sep 2012

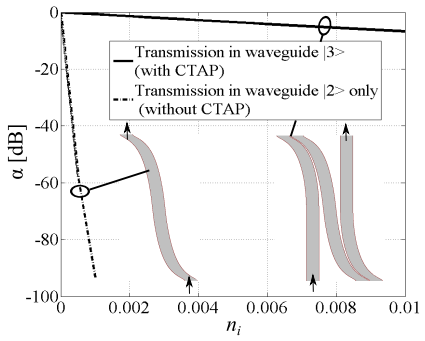

Fig. 3. Power loss (α in decibels) as a function of n_i for the transmission of power through the CTAP structure (solid line) and waveguide $|2\rangle$ only (dash-dot line). The core width of waveguides $|1\rangle, |2\rangle$ and $|3\rangle$ are $w = 2.36$ μm. The arrows for each scenario represent the input (bottom) and output (top) of the optical field.

the CTAP structure is $\alpha_{\text{CTAP}} = -6.70$ dB which represents a relatively low loss given a high material loss index. These small losses can be understood because the CTAP process minimises the power fraction in $|2\rangle$ (see Fig. 2(b)), reducing effective material loss from the 3 waveguide CTAP structure.

3.3. 3-waveguide CTAP - variation in rib heights of waveguides $|2\rangle$ and $|3\rangle$

We now turn to the issue of non-identical waveguides by exploring the role of detuning in the three waveguide model. As mentioned above, the propagation constant is analogous to energy in the CTAP Hamiltonian, and hence variations in β between waveguides plays the same role as detuning. The propagation constant is set by the physical waveguide parameters; refractive index, core width, and rib height. Although variation of the core width would be easiest to realise in practice, the constraint of the mode cutoff and the waveguide separation, does not allow significant detuning. Varying the rib height, although challenging in practice, allows the clearest demonstration of the CTAP method. Hence without loss of generality, we model variations in β by changing rib height. The basic rib height of $h = 1.8$ μm (see Fig. 1(a)) is the optimised height for these CTAP structures with lengths above $L = 4$ mm achieving adiabatic propagation of light. Figure 4 shows the transmission of the CTAP structure as a function of detunings Δ_{21} and Δ_{31}.

In Fig. 4 it can be seen that the CTAP structure can still operate (power fraction $\geq$ 0.9) even when rib height of waveguides $|2\rangle$ and $|3\rangle$ are changed asymmetrically. In particular we find that the system is more robust to Δ_{21} than Δ_{31}, given that the range of operation is greater for Δ_{21} than for Δ_{31}, which means the rib height of waveguide $|2\rangle$ can be changed to a greater extent than waveguide $|3\rangle$ can for operation. Qualitatively Fig. 4 gives the same detuning behaviour as the equivalent scenarios in previous work done for STIRAP (cf. Fig. 10 of [12]), with an asymmetry in the plot occurring along the Δ_{31} axis between -0.02 to 0.03, and for the CTAP of electrons between quantum dots (cf. Fig. 5 of [13]).

3.4. 5-waveguide MRAP - propagation

Here we show the results of a new class of 5-waveguide power divider based on MRAP [20,21]. The propagation of light through the MRAP structure (see Fig. 1(c)) is explored by exciting waveguide $|3\rangle$ with the fundamental mode of the basic waveguide. Figure 5(a) shows the top view (*xz*-plane) of the propagation of light through the MRAP structure. The optical power in

#171934 - $15.00 USD Received 4 Jul 2012; revised 7 Sep 2012; accepted 7 Sep 2012; published 24 Sep 2012

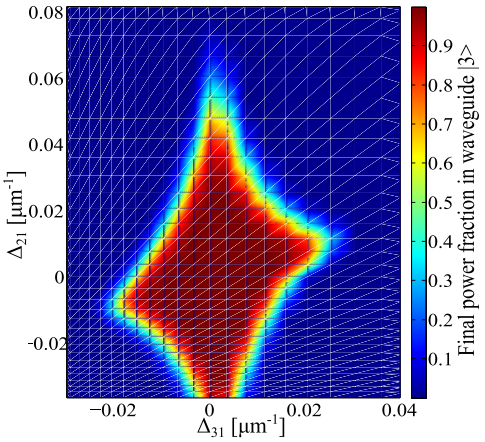

Fig. 4. Power fraction in waveguide $|3\rangle$ at $L = 4$ mm (i.e. end of structure) of the CTAP structure as a function of detunings Δ_{21} and Δ_{31}. Note, $\Delta = 0$ represents no change in the rib height of waveguides $|2\rangle$ and $|3\rangle$. The colour bar shows the final power fraction in $|3\rangle$.

the constituent waveguides as a function of propagation distance z is shown in Fig. 5(b).

Fig. 5. Light propagation (using BeamPROP 8.2 by RSoft Design Group, Inc.) through the MRAP structure, where (a) shows the top view of the structure and the black outlines represent the side walls of the individual waveguides. The grey scale represents the intensity of light, peak is normalised to 1. (b) Power in individual waveguides of $|1\rangle$ (blue line), $|2\rangle$ (red line), $|3\rangle$ (black line), $|4\rangle$ (black dash) and $|5\rangle$ (cyan dash). The fractional powers of waveguides $|2\rangle$ and $|4\rangle$ are multiplied by 100 to make it visible on the scale. Here we have set $\kappa_{\max} = 1.0 \times 10^{-2}$ μm^{-1}, $\kappa_{\min} = 1.0 \times 10^{-5}$ μm^{-1} and $L = 4$ mm.

Figure 5 indicates that light is coupled from the central waveguide of $|3\rangle$ to the outer waveguides of $|1\rangle$ and $|5\rangle$ with minimal excitation of the intermediate waveguides of $|2\rangle$ and $|4\rangle$, showing that light is adiabatically transported via the MRAP process. The power fraction, at the end of the structure, of waveguides $|1\rangle$ and $|5\rangle$ is 0.50. This device represents a new class of power dividers where the power division is robust, as it will be shown in Sec. 3.5, at the level of the ratio of the inter-waveguide couplings, rather than the device length as is the case for usual directional couplers.

#171934 - $15.00 USD Received 4 Jul 2012; revised 7 Sep 2012; accepted 7 Sep 2012; published 24 Sep 2012

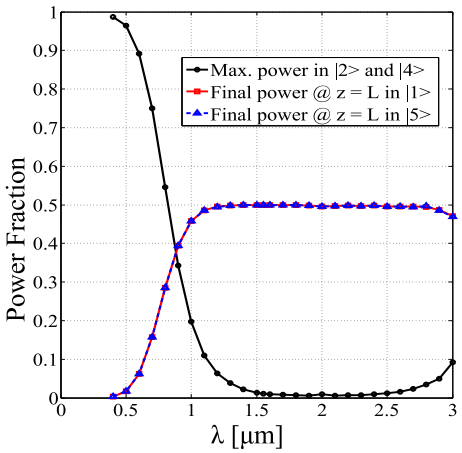

Fig. 6. Spectral response of the MRAP structure, optimised to operate at a wavelength of $\lambda = 1.55$ μm . The solid-dot line represents the summation of the maximum power that occurs in waveguides $|2\rangle$ and $|4\rangle$. The red square-solid (blue triangle-dash) line represents the final power fraction ($L = 4$ mm, i.e., end of structure) of waveguide $|1\rangle$ ($|5\rangle$).

3.5. Spectral study of 5-waveguide MRAP structure

The MRAP structure shown in Sec. 3.4 is optimised for an operation wavelength of $\lambda = 1.55$ μm. To explore the spectral response of the MRAP structure, the wavelength of the input mode in waveguide $|3\rangle$ is swept from 0.4 μm $< \lambda < 3.0$ μm. The quantities of interest are the powers in the individual waveguides. Figure 6 shows the power fraction as a function of input wavelength into the MRAP structure for: the summation of maximum fractional power that occurs in waveguides $|2\rangle$ and $|4\rangle$ (solid-dot line) and final powers occuring at $L = 4$ mm in waveguides $|1\rangle$ (red square-solid line) and $|5\rangle$ (blue triangle-dash line). In the following spectral study of the MRAP structure, material dispersion is not considered. The beam propagation method calculations take into account coupling to higher order modes. Our analysis of the spectral response monitors the power transmitted to the fundamental mode.

Figure 6 shows that the summation of the maximum power that occurs in waveguides $|2\rangle$ and $|4\rangle$ is at a minimum within the range of $1.5 < \lambda < 2.5$ μm (solid-dot line). For waveguides $|1\rangle$ and $|5\rangle$, the output powers at $L = 4$ mm have a 0.5 power fraction within the range of $1.2 < \lambda < 2.8$ μm.

A directional coupler using the same single mode rib waveguides with $\kappa_{\max} = 0.01$ μm^{-1} would permit a $\pi/2$ phase shift between the supermodes in a length of ~ 80 μm, to yield 50% splitting. This is considerably shorter than our device, but with a restricted 1 dB bandwidth of 0.26 μm exhibits an asymmetric splitting ratio away from the centre wavelength. Our device exhibits a 1 dB bandwidth greater than 2 μm with symmetric splitting.

The MRAP structure is an alternative mechanism to achieve a broadband response from an adiabatic passage device, previous work by [18] has also shown an octave spanning 50:50 beamsplitting with a Gaussian coupling scheme via a fractional approach. In each case the robustness of the splitting is due to the fact that it is the ratio of the inter-waveguide coupling rates that is important (providing adiabaticity is satisfied), rather than the absolute value of the coupling, as is the case with directional couplers. This shows that despite the MRAP structure's length, it represents a promising implementation of an ultra-broadband power divider.

#171934 - $15.00 USD Received 4 Jul 2012; revised 7 Sep 2012; accepted 7 Sep 2012; published 24 Sep 2012

4. Conclusion

It has been demonstrated that by using an alternative coupling scheme, the length of a photonic CTAP structure is improved by one order of magnitude compared to previous work. The transmission characteristics of the CTAP structure are robust to perturbations imposed to the optimised system. These included the introduction of material loss and rib height detunings. Even with a high material loss imposed onto waveguide $|2\rangle$, considerable power is transferred through the CTAP structure. The variation in the rib heights introduces an effective detuning to the optimised system. The transmission response as a function of the detunings produced a qualitative equivalence to previous work done in condensed matter CTAP. This qualitative similarity indicates that an analogy can be drawn between optical waveguide and condensed matter CTAP. Extending the ideas from CTAP, the MRAP structure is shown to be a new class of power divider. The MRAP structure exhibits an octave spanning broadband response.

Acknowledgments

The authors would like to thank Jared H. Cole for useful discussion. This work was produced with the assistance of the Australian Research Council (ARC) under the Discovery project scheme (project number DP1096288). S.T-H. is supported by the ARC Australian Research Fellowship (project number DP1096288). A.D.G. is supported by the ARC QEII Fellowship (project number DP0880466).

#171934 - $15.00 USD Received 4 Jul 2012; revised 7 Sep 2012; accepted 7 Sep 2012; published 24 Sep 2012